Transverse momentum balance of dijets in Xe+Xe collisions at the LHC

Yao Li,[1] Shuwan Shen,[1] Sa Wang,[2,*] and Ben-Wei Zhang[1,†]

[1]Key Laboratory of Quark & Lepton Physics (MOE) and Institute of Particle Physics, Central China Normal University, Wuhan 430079, China

[2]Key Laboratory of Atomic and Subatomic Structure and Quantum Control (MOE), Institute of Quantum Matter, South China Normal University, Guangzhou 510006, China

(Dated: January 8, 2024)

We present a theoretical study of the medium modifications on the $p_{\rm T}$ balance ($x_{\rm J}$) of dijets in Xe+Xe collisions at $\sqrt{s_{\rm NN}} = 5.44$ TeV. The initial production of dijets is carried out by the POWHEG+PYTHIA8 prescription, which matches the next-to-leading order (NLO) QCD matrix elements with the parton shower (PS) effect. The in-medium evolution in nucleus-nucleus collisions is described by the SHELL model with a transport approach. The theoretical results of the dijet $x_{\rm J}$ in Xe+Xe collisions exhibit more imbalanced distributions than that in p+p, consistent with the recently reported ATLAS data. By utilizing the Interleaved Flavor Neutralisation, an infrared-and-collinear-safe jet flavor algorithm, to identify the flavor of the reconstructed jets, we classify dijets processes into three categories: gluon-gluon (gg), quark-gluon (qg) and quark-quark (qq), and investigate the respective medium modification patterns and fraction changes of the gg, qg, and qq components of the dijet sample in Xe+Xe collisions. It is shown that the qg component plays a key role in the increased imbalance of the dijet $x_{\rm J}$, and especially the q_1g_2 (quark-jet-leading) dijets experience more significant asymmetric energy loss than the g_1q_2 (gluon-jet-leading) dijets as traversing the QGP. By comparing the $\Delta\langle x_{\rm J}\rangle$ of inclusive, $c\bar{c}$ and $b\bar{b}$ dijets in Xe+Xe collisions, we observe $\Delta\langle x_{\rm J}\rangle_{\rm incl.} > \Delta\langle x_{\rm J}\rangle_{\rm c\bar{c}} > \Delta\langle x_{\rm J}\rangle_{\rm b\bar{b}}$. Moreover, $\rho_{\rm Xe,Pb}$, the ratios of nuclear modification factors of dijets in Xe+Xe to that in Pb+Pb, are calcualted, which indicates that the yield suppression of dijets in Pb+Pb is more pronounced than that in Xe+Xe due to the larger radius of the lead nucleus.

I. INTRODUCTION

The ultra-relativistic heavy-ion collisions at the Large Hadron Collider (LHC) and the Relativistic Heavy Ion Collider (RHIC) provide a unique arena to search for the new form of nuclear matter, the quark-gluon plasma (QGP), in which the degrees of freedom of the quarks and gluons in the protons and neutrons are released [1–5]. The strong interactions between the hard-scattered partons with the medium, referred to as the "jet quenching" phenomenon, open up new avenues to understand the properties of such a fantastic strongly-coupled quark matter [6–9] and test the fundamental theory of quantum chromodynamics (QCD) at the extremely hot and dense conditions [10–16]. In the past two decades, a series of tools have been extensively investigated to reveal this partonic strong interaction, such as the suppression factor $R_{\rm AA}$ of high-$p_{\rm T}$ hadron/jet [17–22], the momentum asymmetry of dijets [23–34], correlations of the vector boson associated jets (γ/Z^0+jets) [35–40], the global event geometry [41, 42] and the jet substructures [43–52].

Since the dijets are the dominant QCD processes in the hadron collisions in the experiment and have less influence from the underlying background, they show a unique glamour in jet physics. In vacuum, the parton shower effects and higher-order QCD processes may break the symmetry of the final-state dijets, which will lead to a deflection from the back-to-back azimuthal angle and an unequal transverse momentum between the leading and subleading jets. In A+A collisions, because the two jets usually experience asymmetric energy loss as traversing the QGP medium, the transverse momentum balance of dijets $x_{\rm J} \equiv p_{\rm T,2}/p_{\rm T,1}$ [53], defined as the ratio of the subleading to leading jet $p_{\rm T}$, can be further modified by the in-medium interactions and show a different sensitivity to the path-length dependence of jet quenching [25] and jet-by-jet fluctuations of jet-medium interactions [54]. And more imbalanced $x_{\rm J}$ distributions of dijets have been observed in Pb+Pb collisions relative to p+p at $\sqrt{s_{\rm NN}} = 2.76$ TeV and $\sqrt{s_{\rm NN}} = 5.02$ TeV by the ATLAS [23, 53, 55] and CMS Collaborations [28, 56, 57], which are extensively investigated by the theoretical calculations [26, 27, 31–34].

Recently, the ATLAS Collaboration has measured the dijet $x_{\rm J}$ in Xe+Xe collisions at $\sqrt{s_{\rm NN}} = 5.44$ TeV for the first time [58], however the timely theoretical studies are still in lack. Because the xenon nucleus has a smaller radius than that of lead, studying the dijet productions in different collision systems will deepen our understanding of the system size dependence of jet quenching effect [53, 55, 59–63]. Furthermore, since the dijet events consist of gg, qg and qq components, while the jet energy loss is closely related to the flavor of hard partons ($\Delta E_g/\Delta E_q \sim C_A/C_F$) [2, 18], it is of significance to figure out their respective modification patterns and assess what roles they played in the overall medium modifications of the dijet $x_{\rm J}$. Furthermore, the massive heavy quarks are believed to lose less energy than the light quarks due to the "dead-cone" effect [64–67], which leads to a mass hierarchy of partonic energy loss $\Delta E_q > \Delta E_c > \Delta E_b$ [49, 68–70]. It is of particular in-

*Electronic address: wangsa@ccnu.edu.cn
†Electronic address: bwzhang@mail.ccnu.edu.cn

terest to explore such mass dependence of the medium modification on the dijet $x_{\rm J}$ by the comparisons between the light- and heavy-flavor (such as $c\bar{c}$ and $b\bar{b}$) dijets in high-energy nuclear collisions.

This paper presents the first theoretical study of medium modifications on the dijet $p_{\rm T}$-balance $x_{\rm J}$ in Xe+Xe collisions. The initial production of dijets is carried out by the POWHEG+PYTHIA8 prescription, which matches the next-to-leading order (NLO) QCD matrix elements with the parton shower (PS) effect. The transport approach describes dijets' in-medium evolution, which considers both the elastic and inelastic partonic interactions in the quark-gluon plasma (QGP). Firstly, we present the theoretical results of the dijet $x_{\rm J}$ in Xe+Xe collisions at $\sqrt{s_{\rm NN}} = 5.44$ TeV compared with the recently reported ATLAS measurements. Specifically, we will discuss the flavor and mass dependence of the medium modification on the dijet $x_{\rm J}$. We study the respective medium modification patterns and fraction changes of the gg, qg, qq, as well as the q_1g_2 and g_1q_2 components in the dijet samples in both p+p and Xe+Xe collisions. We will also investigate the mass effect of the $x_{\rm J}$ modifications by comparing the $\Delta x_{\rm J}$ of inclusive, $c\bar{c}$ and $b\bar{b}$ dijets in Xe+Xe collisions. At last, we present the calculated results of dijets nuclear modification factor in Xe+Xe at $\sqrt{s_{\rm NN}} = 5.44$ TeV and Pb+Pb at $\sqrt{s_{\rm NN}} = 5.02$ TeV compared to the recent ATLAS data.

II. THEORETICAL FRAMEWORK

In this work, we generate the next-to-leading order (NLO) matrix elements for QCD di-jet processes [71] in the framework of POWHEG-BOX-V2 [72–74] and then simulate the parton shower (PS) with PYTHIA 8.309 [75] to produce p+p events. The CT18NLO parton distribution functions (PDF) [76] are chosen in the computation. Jets are reconstructed using the anti-$k_{\rm T}$ clustering algorithm and radius parameter $R = 0.4$ as implemented in the FastJet package [77]. Then, the highest two $p_{\rm T}$ jets out of the set of jets in an event are selected as the dijet candidate. The leading jet transverse momentum $p_{\rm T,1}$ and subleading jet transverse momentum $p_{\rm T,2}$ are required to be greater than 100 GeV/c and 32 GeV/c, respectively. The two jets are required to be nearly back-to-back in azimuth with $\Delta\phi \equiv |\phi_1 - \phi_2| \geq 7\pi/8$ and to be in the rapidity region $|y| < 2.1$. If all these conditions are met, the desired dijet candidate is accepted.

We calculate the normalized $x_{\rm J}$ distributions in p+p collisions and compare that to the ATLAS data [55] as shown in Fig. 1. We observe that the $x_{\rm J}$ distributions calculated by POWHEG+PYTHIA8 give decent descriptions at small value of $x_{\rm J}$ for all six different $p_{\rm T,1}$ intervals compared to the ATLAS data, except for a little overestimation of $x_{\rm J}$ distributions than the ATLAS data near 1. At each $p_{\rm T}$ interval, the $x_{\rm J}$ distribution peaks near $x_{\rm J} \simeq 1$, where the leading and subleading jets are almost balanced. However, with the higher-order perturbative QCD corrections and the splitting processes during the parton shower in vacuum, a considerable fraction of dijets are produced with imbalanced transverse momentum at the smaller $x_{\rm J}$ region.

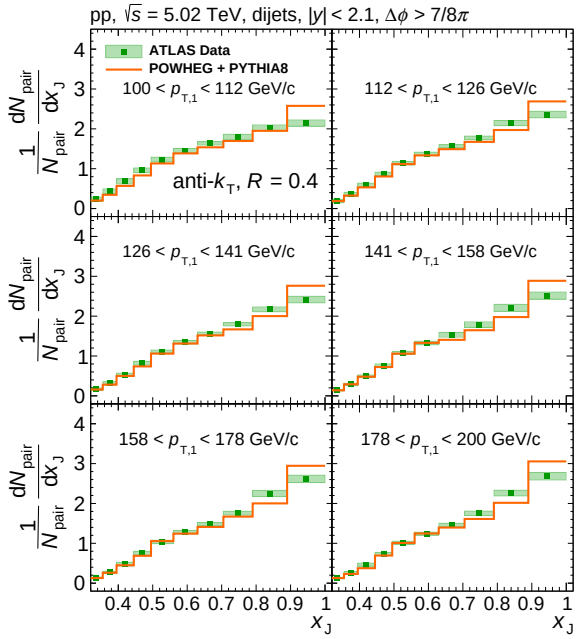

FIG. 1: (Color online) Normalized $x_{\rm J}$ distributions of dijets in p+p collisions at $\sqrt{s} = 5.02$ TeV for six $p_{\rm T,1}$ intervals: [100, 112], [112, 126], [126, 141], [141, 158], [158, 171] and [171, 200] GeV/c are compared with the ATLAS data [55].

The in-medium evolution of both light- and heavy-flavor dijets are simulated by the SHELL model [34, 78–85], which takes into account the elastic and inelastic partonic energy loss within the hot/dense QGP medium. Since the propagation of massive partons in the QCD medium can be viewed as "Brownian motion", the transport of heavy quarks can be well described by the modified Langevin equations,

$$\Delta\vec{x}(t) = \frac{\vec{p}(t)}{E}\Delta t, \tag{1}$$

$$\Delta\vec{p}(t) = -\eta_D\vec{p}\Delta t + \vec{\xi}(t)\Delta t - \vec{p}_{\rm g}(t). \tag{2}$$

These two equations describe heavy quarks' position and momentum updates as traversing the QGP medium. η_D is the drag coefficient controlling the energy dissipation strength of heavy quarks in the medium. The stochastic term $\xi(t)$ denotes the random kicks as heavy quarks scatter with the thermal particle, which obeys a Gaussian distribution. The diffusion coefficient κ could be related to the η_D by the fluctuation-dissipation theorem $\kappa = 2\eta_D ET$. Note that the first two terms at the right-hand side of Eq. 2 represent the collisional energy loss of heavy quarks. In contrast, the last term $-p_g$ is the momentum correction caused by the medium-induced gluon radiation. In our framework, the Higher-Twist [65, 86–88] formalism has been employed to simulate the medium-induced gluon radiation of jet partons, in which

the gluon radiation spectra of an energetic parton in the QGP can be obtained,

$$\frac{dN_g}{dxdk_\perp^2 dt} = \frac{2\alpha_s P(x)\hat{q}}{\pi k_\perp^4}\sin^2\left(\frac{t-t_i}{2\tau_f}\right)\left(\frac{k_\perp^2}{k_\perp^2+x^2M^2}\right)^4, \quad (3)$$

where x and $k_\perp$ denote the radiated gluon's energy fraction and transverse momentum. $P(x)$ is the QCD splitting function for the splitting processes $g \to g+g$ and $q(Q) \to q(Q)+g$ [89], $\tau_f = 2Ex(1-x)/(k_\perp^2+x^2M^2)$ the formation time of the daughter gluon. $\hat{q}$ denotes the general jet transport parameter in the QGP [90]. The last term in Eq. 3 represents the suppression factor results from the "dead-cone" effect of heavy quarks [64, 91], which suppresses the probability of gluon radiation within a small cone ($\theta \sim M_Q/E$). The collisional energy loss is generally dominant for low-energy heavy quarks due to the "dead-cone" effect. In contrast, the radiative energy loss is usually expected to become significant at $p_{\rm T}^Q > 5m_Q$ [92]. For massless partons, the collisional energy loss is estimated by the pQCD calculations within the Hard-Thermal Loop approximation [93, 94], while their radiative contribution by the same Higher-Twist formalism as for massive partons. The hydrodynamics time-space evolution of the QGP medium is described by the CLVisc programs [95, 96], which provides the temperature and velocity of the expanding hot/dense nuclear matter. The SHELL model has been successfully applied in the study of heavy-flavor jets in high-energy nuclear collisions, which gives satisfactory descriptions on a series of experiment measurements, such as $p_{\rm T}$ imbalance [34], radial profiles [78–80] and fragmentation functions [84] of heavy-flavor jets, correlations of Z^0+ HF hadron/jet [82, 83].

III. NUMERICAL RESULTS AND DISCUSSIONS

In Fig. 2(a), we firstly show the dijet $x_{\rm J}$ distributions in Xe+Xe collisions at $\sqrt{s_{\rm NN}} = 5.44$ TeV calculated by the SHELL model as a comparison to the ATLAS data for four centrality bins ($0-10\%$, $10\%-20\%$, $20\%-40\%$ and $40\%-80\%$) and two $p_{\rm T,1}$ intervals ([100, 126] GeV/c and [158, 199] GeV/c). We find that the calculations by the SHELL model give a satisfactory description of the recently reported ATLAS data for almost all four centrality bins and two $p_{\rm T,1}$ intervals, only overestimate the data at $x_{\rm J} \sim 1$ for $158 < p_{\rm T,1} < 199$ GeV/c in the central $0-10\%$ collisions. Furthermore, our theoretical results show a more balanced $x_{\rm J}$ distribution for higher $p_{\rm T}$ dijets ($158 < p_{\rm T,1} < 199$ GeV/c) than the lower one, which is consistent with the trend observed in the ATLAS measurements. To figure out the collision centrality and jet $p_{\rm T}$ dependence of the medium modification on the dijet $x_{\rm J}$ distributions, we also compare the dijet $x_{\rm J}$ distributions in Xe+Xe collisions with their p+p baseline for two $p_{\rm T}$ intervals as shown in Fig. 2(b), and the ratios of XeXe/pp are shown in the bottom panels. The $x_{\rm J}$ distributions are observed to shift towards smaller $x_{\rm J}$ values

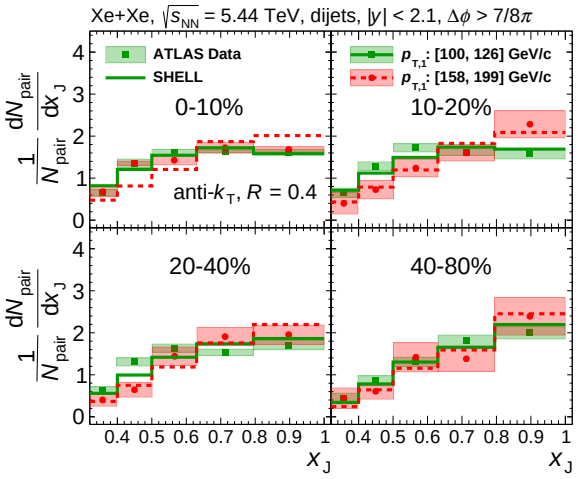

(a)

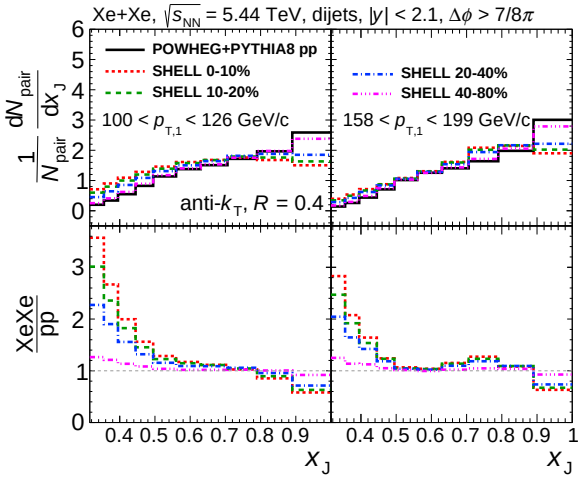

(b)

FIG. 2: (Color online) (a) Calculated normalized dijet $x_{\rm J}$ distributions in Xe+Xe collisions at $\sqrt{s_{\rm NN}} = 5.44$ TeV are compared with the ATLAS data for four centrality bins ($0-10\%$, $10\%-20\%$, $20\%-40\%$ and $40\%-80\%$) and two $p_{\rm T,1}$ intervals (green: [100, 126] GeV/c, red: [158, 199] GeV/c). (b) Comparisons of the normalized dijets $x_{\rm J}$ distributions between Xe+Xe and p+p collisions at $\sqrt{s_{\rm NN}} = 5.44$ TeV for two $p_{\rm T,1}$ intervals (left: [100, 126] GeV/c, right: [158, 199] GeV/c), and the ratios of XeXe/pp are shown in the bottom panels.

in Xe+Xe collisions compared to their p+p baseline, especially for the most central collisions. The phenomenon that the dijet transverse momentum gets more imbalanced in A+A collisions due to the asymmetric energy loss suffered on the leading and subleading jets as the dijet traversing the QGP [25, 54] has been observed by the previous measurements in Pb+Pb collisions at 2.76 TeV [53] and 5.02 TeV [55]. In the central collisions, such asymmetric energy loss between the leading and subleading jets can be more significant due to the larger medium size and higher temperature than the peripheral case. In addition, we observe slightly weaker $x_{\rm J}$ modification for higher $p_{\rm T}$ dijets than the lower one, which is consistent

with the expected. We can imagine that the $x_{\rm J}$ of dijets with very high $p_{\rm T}$ is relatively difficult to be influenced by the medium effects compared to the one with low $p_{\rm T}$.

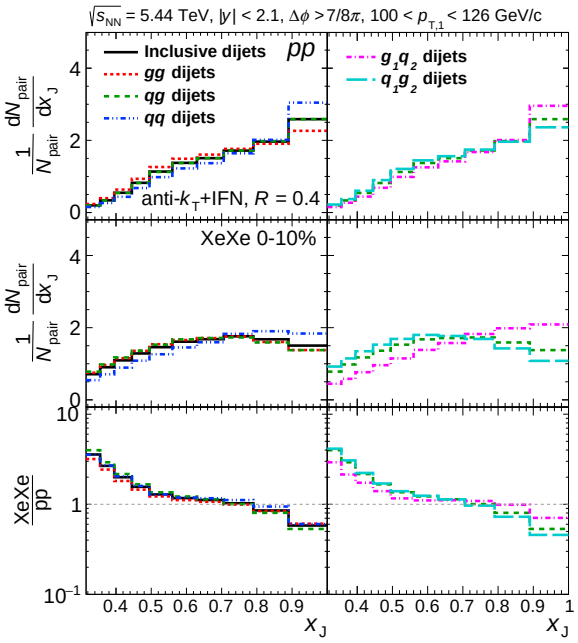

FIG. 3: (Color online) Calculated normalized $x_{\rm J}$ distributions in p+p (top) and $0-10\%$ Xe+Xe (middle) collisions as well as their ratios (bottom) for: inclusive, gluon-gluon, quark-gluon, and quark-quark dijets (left column); quark-jet-leading and gluon-jet-leading of quark-gluon dijets (right column). The $x_{\rm J}$ distributions of quark-gluon dijets (dashed green line) in the right column are the same as in the left column.

The flavor dependence of the medium modification of dijet $p_{\rm T}$ balance is also an interesting topic in heavy-ion collisions. Due to the different color factors ($C_A = 3$ for gluons, $C_F = 4/3$ for quarks), the gluon-initiated jets are expected to lose more energy than the quark-initiated one as traversing the hot and dense nuclear matter, and the "dead-cone" effect also leads to smaller energy loss of heavy quarks than that of the light one [2, 18, 64–67]. An optimal step toward this goal is determining the flavor of the selected jets in nucleus-nucleus collisions with an infrared and collinear (IRC) safe jet algorithm. In recent years, four IRC-safe jet-algorithm-based approaches have been developed to identify the flavor of the underlying hard partons for the final-state reconstructed jets, called "flavor-$k_{\rm T}$" [97], "flavor anti-$k_{\rm T}$" [98], "flavor-dressing" [99] and "Interleaved Flavor Neutralisation (IFN)" [100]. In this work, we employ the IFN algorithm to identify the flavor of the reconstructed jets at parton level for the gluon-jets, light-quark jets and the heavy-flavor jets in both p+p and nucleus-nucleus collisions. Note that, since the flavor information of the jets is accessible at each stage of the clustering sequence, the IFN algorithm provides a consistent flavor identification both to the full jets and their substructures.

By utilizing the IFN algorithm, the inclusive dijet events can be classified into three categories: gluon-gluon (gg), quark-gluon (qg), and quark-quark (qq). In particular, by distinguishing the flavor of the leading jet, the qg dijets can be further divided into q_1g_2 and g_1q_2, denoting the quark-jet-leading and gluon-jet-leading quark-gluon dijets, respectively. In the left column of Fig. 3, we show the normalized $x_{\rm J}$ distributions of gg, qg, qq, and inclusive dijets in both p+p and $0-10\%$ Xe+Xe collisions at $\sqrt{s_{\rm NN}} = 5.44$ TeV, and the ratio of XeXe/pp is plotted in the bottom panel. We find that gg dijets have a more imbalanced initial distribution than qq. Quark and gluon experience different parton shower processes in vacuum due to their different color factors and splitting functions [75, 101]. In the bottom panel, it is observed that the qq and gg dijets have almost the same medium modification, while the qg dijets have the stronger suppression near $x_{\rm J} \sim 1$ and enhancement near $x_{\rm J} \sim 0$ than the others. The different color charge carried by the leading and subleading jets of qg dijets leads to enhanced asymmetric energy loss in Xe+Xe collisions relative to the qq and gg one. However, we note that the qg dijets contain two types of subsets, q_1g_2 and g_1q_2, which may have different modification patterns. In the right column of Fig. 3, we observe stronger enhancement at small $x_{\rm J}$ and also stronger suppression at $x_{\rm J} \sim 1$ on the $x_{\rm J}$ distribution of q_1g_2 dijets than that of g_1q_2. Compared to the g_1q_2 dijets, the leading jet of q_1g_2 dijets loses less energy while the subleading one loses more. In other words, the flavor configuration of q_1g_2 dijets makes them experience more significant asymmetric energy loss than g_1q_2 as traversing the QGP medium.

On the other hand, we also estimate the component fractions of dijet sample in p+p and $0-10\%$ Xe+Xe collisions at $\sqrt{s_{\rm NN}} = 5.44$ TeV shown in Fig. 4, which would be helpful to understand the role of jet flavor played in the jet-medium interactions. In the left column, we show the fractions of gg, qg, and qq in the inclusive dijets in p+p (top) and Xe+Xe (middle) collisions, as well as their differences (bottom). Firstly, we find that the qg has the most prominent initial fraction ($\sim 50\%$) in p+p collisions, and the fraction is increased at small $x_{\rm J}$ but reduced at $x_{\rm J} \sim 1$ in Xe+Xe collisions. Second, the fraction of gg is overall reduced. At the same time, that of qq is enhanced because, generally, the gg dijets lose more energy, which makes it more difficult to survive in jet selection relative to qq. Since the qg has the most significant fraction in the dijet sample, the enhanced fractions of qg at small $x_{\rm J}$ in Xe+Xe is the key point that leads to the increased $p_{\rm T}$ imbalance of inclusive dijets. Furthermore, it is essential to address the fraction changes of the q_1g_2 and g_1q_2 subsets in A+A collisions. In the right column of Fig. 4, it is observed that the fractions of q_1g_2 and g_1q_2 have opposite behaviors in Xe+Xe collisions compared to their initial values. The fraction of q_1g_2 is significantly enhanced at small $x_{\rm J}$ after traversing the QGP, while that of g_1q_2 is decreased at this region.

To quantify the overall shift of the $x_{\rm J}$ distribution in Xe+Xe collisions relative to p+p, we calculate the average values ($\langle x_{\rm J} \rangle$) of dijet $x_{\rm J}$ distributions and their differ-

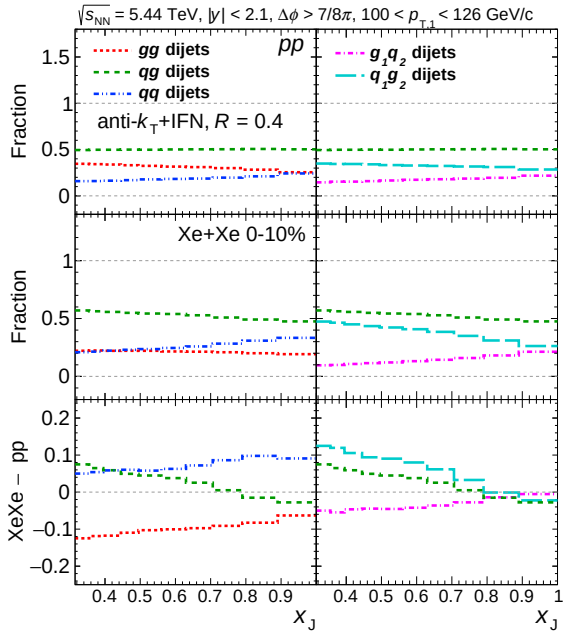

FIG. 4: (Color online) Calculated fraction of subset dijets in inclusive dijets as the function of $x_{\rm J}$ in p+p (top) and 0−10% Xe+Xe (middle) collisions as well as their differences (bottom) for: gluon-gluon, quark-gluon, and quark-quark dijets (left column); quark-jet-leading and gluon-jet-leading quark-gluon dijets (right column). The fraction distributions of quark-gluon dijets in the right column (dashed green line) are the same as in the left column.

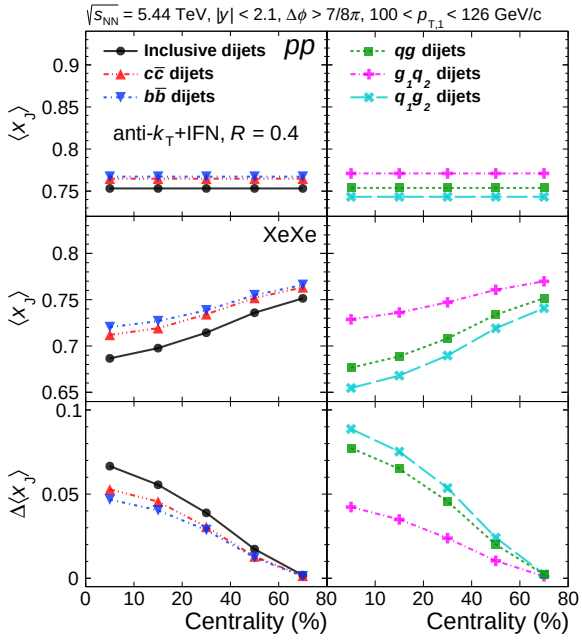

FIG. 5: (Color online) Averaged $x_{\rm J}$ of the inclusive, $c\bar{c}$, $b\bar{b}$ dijets (left) and q_1g_2, g_1q_2, qg dijets (right) in p+p (top) and Xe+Xe (middle) collisions as a function of the collision centrality, as well as their differences $\Delta\langle x_{\rm J}\rangle$ (bottom).

ences ($\Delta\langle x_{\rm J}\rangle$) between p+p and A+A collisions, defined as follows

$$\langle x_{\rm J}\rangle \equiv \int \frac{1}{N_{\rm pair}}\frac{dN_{\rm pair}}{dx_{\rm J}}x_{\rm J}dx_{\rm J}, \tag{4}$$

$$\Delta\langle x_{\rm J}\rangle = \langle x_{\rm J}\rangle_{\rm pp} - \langle x_{\rm J}\rangle_{\rm AA}. \tag{5}$$

To address the mass dependence of the medium modification of dijet $x_{\rm J}$, in the left column of Fig. 5 we show the $\langle x_{\rm J}\rangle$ of inclusive, $c\bar{c}$ and $b\bar{b}$ dijets in p+p and Xe+Xe collisions as a function of centrality, as well as their differences $\Delta\langle x_{\rm J}\rangle$. We find that $\Delta\langle x_{\rm J}\rangle$ decreases monotonously from central to peripheral collisions, as we found in Fig. 2(b). It is also observed that the $\Delta\langle x_{\rm J}\rangle$ of these three kinds of dijets obey the hierarchy $\Delta\langle x_{\rm J}\rangle_{\rm incl.} > \Delta\langle x_{\rm J}\rangle_{c\bar{c}} > \Delta\langle x_{\rm J}\rangle_{b\bar{b}}$ in Xe+Xe collisions for the same centrality bin. It indicates that the massive dijets suffer less asymmetric energy loss in A+A collisions than the massless light flavor one. The future measurements focusing on these comparisons will help test the mass effect of jet energy loss. In the right column of Fig. 5, $\Delta\langle x_{\rm J}\rangle$ of q_1g_2 and g_1q_2 dijets in Xe+Xe are also plotted, and the former has significantly large values than the latter for each centrality bin.

To quantitatively characterize the relative dijet yield suppression between Xe+Xe and Pb+Pb collisions, the nuclear-modification factors for leading jets, $\rho_{\rm Xe,Pb}(p_{\rm T,1})$ is defined as follows (similarly, $\rho_{\rm Xe,Pb}(p_{\rm T,2})$ can be defined for subleading jets)

$$R_{\rm AA}(p_{\rm T,1}) = \frac{1}{\langle T_{\rm AA}\rangle}\frac{d\sigma^{\rm pair}_{\rm AA}/dp_{\rm T,1}}{d\sigma^{\rm pair}_{pp}/dp_{\rm T,1}}, \tag{6}$$

$$\rho_{\rm Xe,Pb}(p_{\rm T,1}) = \frac{R_{\rm XeXe}(p_{\rm T,1})}{R_{\rm PbPb}(p_{\rm T,1})}. \tag{7}$$

In Fig. 6, we show the calculated $\rho_{\rm Xe,Pb}(p_{\rm T,1})$ (left) and $\rho_{\rm Xe,Pb}(p_{\rm T,2})$ (right) of dijets for three centrality bins: 0 − 10%, 10% − 20% and 20% − 40%. Note that we use a cut $x_{\rm J} > 0.32$ in the calculation to be consistent with ATLAS's treatment in the measurements. We observe that the values of $\rho_{\rm Xe,Pb}$ are generally larger than one for both leading and subleading jets for all centrality bins. It indicates a weaker yield suppression of dijets in Xe+Xe collisions than that in Pb+Pb for the same centrality bin, and this phenomenon is still evident even at peripheral collisions. These findings are consistent with the previous phenomenological studies [61–63]. Since the nucleus of xenon has a smaller radius than that of lead, the system size and the mean temperature of the QGP medium formed in Xe+Xe collisions is expected to be smaller than that in Pb+Pb collisions within the same centrality interval [85]. Hence, dijets traverse a longer path-length medium and experience more effective energy loss in Pb+Pb collisions.

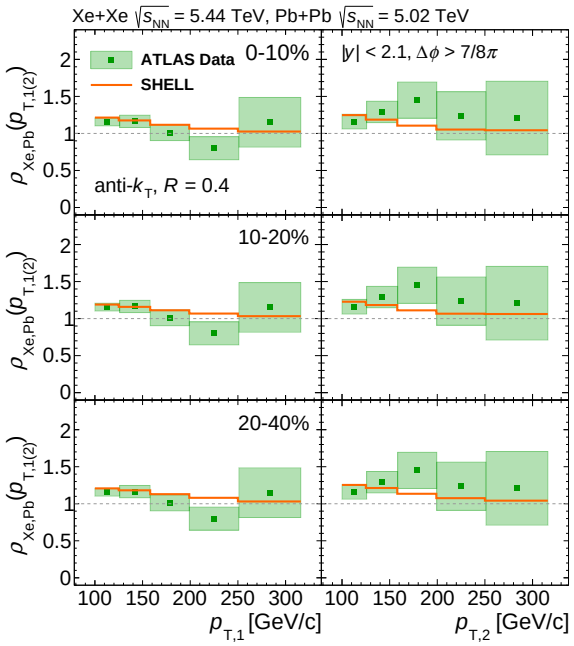

FIG. 6: (Color online) Calculated ratios of Xe+Xe and Pb+Pb pair nuclear modification factors, $\rho_{\rm Xe,Pb}$, evaluated as a function of $p_{\rm T,1}$ (left) and $p_{\rm T,2}$ (right) in the same centrality intervals, and compared to the ATLAS data.

IV. CONCLUSION

In this paper, we present the first investigation on the medium modifications of dijet $p_{\rm T}$ balance ($x_{\rm J}$) in Xe+Xe collisions at $\sqrt{s_{\rm NN}}$ = 5.44 TeV. The initial $x_{\rm J}$ distributions of dijets are calculated by the POWHEG+PYTHIA8 prescription, which matches the NLO QCD matrix elements with the parton shower effect. The in-medium evolution of dijets in nucleus-nucleus collisions is described by the SHELL model, which considers both the elastic and inelastic partonic interactions in the quark-gluon plasma (QGP). Our theoretical results of the dijet $x_{\rm J}$ in Xe+Xe collisions exhibit a more imbalanced distribution than that in p+p, consistent with the recently reported ATLAS data. The dijet becomes increasingly imbalanced from peripheral to central Xe+Xe collisions, consistent with the previous measurements in Pb+Pb collisions at the LHC. Furthermore, with the help of an infrared-and-collinear-safe flavor jet algorithm, we explore the flavor dependence of medium modification of dijet $p_{\rm T}$ balance in nucleus-nucleus collisions. We study the respective medium modification patterns and fraction changes of the gg, qg, and qq components in the dijet sample in both p+p and Xe+Xe collisions. We demonstrate that the qg component plays a key role in the increased imbalance of the dijet $x_{\rm J}$. Especially we find that the q_1g_2 dijets experience more significant asymmetric energy loss than the g_1q_2 dijets as traversing the QGP. By comparing the $\Delta\langle x_{\rm J}\rangle$ of inclusive, $c\bar{c}$ and $b\bar{b}$ dijets in Xe+Xe collisions, we observe $\Delta\langle x_{\rm J}\rangle_{\rm incl.} > \Delta\langle x_{\rm J}\rangle_{\rm c\bar{c}} > \Delta\langle x_{\rm J}\rangle_{\rm b\bar{b}}$ consistent with the mass hierarchy of partonic energy loss. In addition, our calculated nuclear modification factor $\rho_{\rm Xe,Pb}$ of dijets in Xe+Xe at $\sqrt{s_{\rm NN}}$ = 5.44 TeV and Pb+Pb at $\sqrt{s_{\rm NN}}$ = 5.02 TeV are consistent with the ATLAS data, which indicates that the yield suppression of dijets in Pb+Pb is more pronounced than that in Xe+Xe due to the larger radius of the lead nucleus.

Acknowledgments: This research is supported by the Guangdong Major Project of Basic and Applied Basic Research No. 2020B0301030008, and the National Natural Science Foundation of China with Project Nos. 11935007, 12035007, 12247127 and 12247132. S. Wang is supported by China Postdoctoral Science Foundation under project No. 2021M701279.

[1] X. N. Wang and M. Gyulassy, Phys. Rev. Lett. 68, 1480-1483 (1992).
[2] M. Gyulassy, I. Vitev, X. N. Wang and B. W. Zhang, In *Hwa, R.C. (ed.) et al.: Quark gluon plasma* 123-191
[3] Y. Mehtar-Tani, J. G. Milhano and K. Tywoniuk, Int. J. Mod. Phys. A 28, 1340013 (2013) [arXiv:1302.2579 [hep-ph]].
[4] G. Y. Qin and X. N. Wang, Int. J. Mod. Phys. E 24, no. 11, 1530014 (2015).
[5] E. Wang and X. N. Wang, Phys. Rev. Lett. 87, 142301 (2001) [arXiv:nucl-th/0106043 [nucl-th]].
[6] K. M. Burke et al. [JET], Phys. Rev. C 90 (2014) no.1, 014909 [arXiv:1312.5003 [nucl-th]].
[7] M. Xie, W. Ke, H. Zhang and X. N. Wang, Phys. Rev. C 108 (2023) no.1, L011901 [arXiv:2206.01340 [hep-ph]].
[8] H. X. Zhang, Y. X. Xiao, J. W. Kang and B. W. Zhang, Nucl. Sci. Tech. 33 (2022) no.11, 150 [arXiv:2102.11792 [hep-ph]].
[9] D. Everett et al. [JETSCAPE], Phys. Rev. C 103 (2021) no.5, 054904 [arXiv:2011.01430 [hep-ph]].
[10] L. Cunqueiro and A. M. Sickles, Prog. Part. Nucl. Phys. 124, 103940 (2022) [arXiv:2110.14490 [nucl-ex]].
[11] S. Cao and X. N. Wang, Rept. Prog. Phys. 84 (2021) no.2, 024301 [arXiv:2002.04028 [hep-ph]].
[12] J. C. Collins and M. J. Perry, Phys. Rev. Lett. 34, 1353 (1975)
[13] Z. Tang, Z. B. Tang, W. Zha, W. M. Zha, Y. Zhang and Y. F. Zhang, Nucl. Sci. Tech. 31 (2020) no.8, 81 [arXiv:2105.11656 [nucl-ex]].
[14] C. Shen and L. Yan, Nucl. Sci. Tech. 31 no.12, 122 [arXiv:2010.12377 [nucl-th]].
[15] C. Liu, X. G. Deng and Y. G. Ma, Nucl. Sci. Tech. 33 (2022) no.5, 52
[16] J. H. Gao, G. L. Ma, S. Pu and Q. Wang, Nucl. Sci. Tech. 31 (2020) no.9, 90 [arXiv:2005.10432 [hep-ph]].
[17] G. Aad et al. [ATLAS], Phys. Rev. Lett. 114 (2015) no.7, 072302 [arXiv:1411.2357 [hep-ex]].
[18] X. N. Wang, Phys. Rev. C 58, 2321 (1998) [arXiv:hep-ph/9804357 [hep-ph]].
[19] S. A. Bass, C. Gale, A. Majumder, C. Nonaka,

G. Y. Qin, T. Renk and J. Ruppert, Phys. Rev. C 79 (2009), 024901 [arXiv:0808.0908 [nucl-th]].
[20] E. Wang and X. N. Wang, Phys. Rev. Lett. 89, 162301 (2002) [arXiv:hep-ph/0202105 [hep-ph]].
[21] S. Cao et al. [JETSCAPE], Phys. Rev. C 104 (2021) no.2, 024905 [arXiv:2102.11337 [nucl-th]].
[22] Y. He, S. Cao, W. Chen, T. Luo, L. G. Pang and X. N. Wang, Phys. Rev. C 99 (2019) no.5, 054911 [arXiv:1809.02525 [nucl-th]].
[23] G. Aad et al. [ATLAS], Phys. Rev. Lett. 105 (2010), 252303 [arXiv:1011.6182 [hep-ex]].
[24] H. Zhang, J. F. Owens, E. Wang and X. N. Wang, Phys. Rev. Lett. 98 (2007), 212301 [arXiv:nucl-th/0701045 [nucl-th]].
[25] G. Y. Qin and B. Muller, Phys. Rev. Lett. 106 (2011), 162302 [erratum: Phys. Rev. Lett. 108 (2012), 189904] [arXiv:1012.5280 [hep-ph]].
[26] F. Senzel, O. Fochler, J. Uphoff, Z. Xu and C. Greiner, J. Phys. G 42 (2015) no.11, 115104 [arXiv:1309.1657 [hep-ph]].
[27] Z. B. Kang, J. Reiten, I. Vitev and B. Yoon, Phys. Rev. D 99 (2019) no.3, 034006 [arXiv:1810.10007 [hep-ph]].
[28] I. V. Fialkovsky, V. N. Marachevsky and D. V. Vassilevich, Phys. Rev. B 84 (2011), 035446 [arXiv:1102.1757 [hep-th]].
[29] H. Xing, Z. B. Kang, I. Vitev and E. Wang, Phys. Rev. D 86 (2012), 094010 [arXiv:1206.1826 [hep-ph]].
[30] Z. B. Kang, I. Vitev and H. Xing, Phys. Rev. D 85 (2012), 054024 [arXiv:1112.6021 [hep-ph]].
[31] Z. Gao, A. Luo, G. L. Ma, G. Y. Qin and H. Z. Zhang, Phys. Rev. C 97 (2018) no.4, 044903 [arXiv:1612.02548 [hep-ph]].
[32] T. Renk, Phys. Rev. C 86 (2012), 061901 [arXiv:1204.5572 [hep-ph]].
[33] L. Chen, G. Y. Qin, S. Y. Wei, B. W. Xiao and H. Z. Zhang, Phys. Lett. B 782 (2018), 773-778 [arXiv:1612.04202 [hep-ph]].
[34] W. Dai, S. Wang, S. L. Zhang, B. W. Zhang and E. Wang, Chin. Phys. C 44 (2020), 104105 [arXiv:1806.06332 [nucl-th]].
[35] S. Chatrchyan et al. [CMS], Phys. Lett. B 718 (2013), 773-794 [arXiv:1205.0206 [nucl-ex]].
[36] R. B. Neufeld, I. Vitev and B.-W. Zhang, Phys. Rev. C 83, 034902 (2011). [arXiv:1006.2389 [hep-ph]].
[37] W. Dai, I. Vitev and B. W. Zhang, Phys. Rev. Lett. 110 (2013) no.14, 142001 [arXiv:1207.5177 [hep-ph]].
[38] J. Huang, Z. B. Kang, I. Vitev and H. Xing, Phys. Lett. B 750 (2015), 287-293 [arXiv:1505.03517 [hep-ph]].
[39] Z. Yang, T. Luo, W. Chen, L. G. Pang and X. N. Wang, Phys. Rev. Lett. 130 (2023) no.5, 052301 [arXiv:2203.03683 [hep-ph]].
[40] W. Chen, S. Cao, T. Luo, L. G. Pang and X. N. Wang, Phys. Lett. B 810 (2020), 135783 [arXiv:2005.09678 [hep-ph]].
[41] S. Y. Chen, W. Dai, S. L. Zhang, Q. Zhang and B. W. Zhang, Eur. Phys. J. C 80 (2020) no.9, 865 [arXiv:2005.02892 [hep-ph]].
[42] J. W. Kang, L. Wang, W. Dai, S. Wang and B. W. Zhang, [arXiv:2304.04649 [nucl-th]].
[43] S. Chatrchyan et al. [CMS], Phys. Lett. B 730 (2014), 243-263 [arXiv:1310.0878 [nucl-ex]].
[44] I. Vitev and B. W. Zhang, Phys. Rev. Lett. 104, 132001 (2010). [arXiv:0910.1090 [hep-ph]].
[45] I. Vitev, S. Wicks and B. W. Zhang, JHEP 0811, 093 (2008).
[46] S. L. Zhang, M. Q. Yang and B. W. Zhang, Eur. Phys. J. C 82 (2022) no.5, 414 [arXiv:2105.04955 [hep-ph]].
[47] S. Y. Chen, J. Yan, W. Dai, B. W. Zhang and E. Wang, Chin. Phys. C 46 (2022) no.10, 104102 [arXiv:2204.01211 [hep-ph]].
[48] S. L. Zhang, T. Luo, X. N. Wang and B. W. Zhang, Phys. Rev. C 98 (2018), 021901 [arXiv:1804.11041 [nucl-th]].
[49] S. Wang, W. Dai, E. Wang, X. N. Wang and B. W. Zhang, Symmetry 15 (2023) no.3, 727 [arXiv:2303.14660 [nucl-th]].
[50] Y. Tachibana et al. [JETSCAPE], [arXiv:2301.02485 [hep-ph]].
[51] L. Wang, J. W. Kang, Q. Zhang, S. Shen, W. Dai, B. W. Zhang and E. Wang, Chin. Phys. Lett. 40 (2023) no.3, 032101 [arXiv:2211.13674 [nucl-th]].
[52] J. W. Kang, S. Wang, L. Wang and B. W. Zhang, [arXiv:2312.15518 [hep-ph]].
[53] M. Aaboud et al. [ATLAS], Phys. Lett. B 774 (2017), 379-402 [arXiv:1706.09363 [hep-ex]].
[54] J. G. Milhano and K. C. Zapp, Eur. Phys. J. C 76 (2016) no.5, 288 [arXiv:1512.08107 [hep-ph]].
[55] G. Aad et al. [ATLAS], Phys. Rev. C 107 (2023) no.5, 054908 [arXiv:2205.00682 [nucl-ex]].
[56] S. Chatrchyan et al. [CMS], Phys. Lett. B 712 (2012), 176-197 [arXiv:1202.5022 [nucl-ex]].
[57] A. M. Sirunyan et al. [CMS], JHEP 03 (2018), 181 [arXiv:1802.00707 [hep-ex]].
[58] G. Aad et al. [ATLAS], Phys. Rev. C 108 (2023) no.2, 024906 [arXiv:2302.03967 [nucl-ex]].
[59] S. Acharya et al. [ALICE], Phys. Lett. B 788 (2019), 166-179 [arXiv:1805.04399 [nucl-ex]].
[60] G. Aad et al. [ATLAS], Phys. Rev. C 101 (2020) no.2, 024906 [arXiv:1911.04812 [nucl-ex]].
[61] M. Xie, S. Y. Wei, G. Y. Qin and H. Z. Zhang, Eur. Phys. J. C 79 (2019) no.7, 589 [arXiv:1901.04155 [hep-ph]].
[62] S. Q. Li, W. J. Xing, X. Y. Wu, S. Cao and G. Y. Qin, Eur. Phys. J. C 81 (2021) no.11, 1035 [arXiv:2108.06648 [hep-ph]].
[63] Q. Zhang, W. Dai, L. Wang, B. W. Zhang and E. Wang, Chin. Phys. C 46 (2022) no.10, 104106 [arXiv:2203.10742 [hep-ph]].
[64] Y. L. Dokshitzer and D. E. Kharzeev, Phys. Lett. B 519 (2001), 199-206 [arXiv:hep-ph/0106202 [hep-ph]].
[65] B. W. Zhang, E. Wang and X. N. Wang, Phys. Rev. Lett. 93, 072301 (2004) [arXiv:nucl-th/0309040 [nucl-th]].
[66] N. Armesto, C. A. Salgado and U. A. Wiedemann, Phys. Rev. D 69 (2004), 114003 [arXiv:hep-ph/0312106 [hep-ph]].
[67] M. Djordjevic and M. Gyulassy, Phys. Lett. B 560 (2003), 37-43 [arXiv:nucl-th/0302069 [nucl-th]].
[68] W. J. Xing, S. Cao, G. Y. Qin and H. Xing, Phys. Lett. B 805 (2020), 135424 [arXiv:1906.00413 [hep-ph]].
[69] W. J. Xing, S. Cao and G. Y. Qin, [arXiv:2303.12485 [hep-ph]].
[70] S. L. Zhang, E. Wang, H. Xing and B. W. Zhang, [arXiv:2303.14881 [hep-ph]].
[71] S. Alioli, K. Hamilton, P. Nason, C. Oleari and E. Re, JHEP 04, 081 (2011) [arXiv:1012.3380 [hep-ph]].
[72] P. Nason, JHEP 11, 040 (2004) [arXiv:hep-ph/0409146 [hep-ph]].
[73] S. Frixione, P. Nason and C. Oleari, JHEP 11, 070 (2007) [arXiv:0709.2092 [hep-ph]].

[74] S. Alioli, P. Nason, C. Oleari and E. Re, JHEP 06, 043 (2010) [arXiv:1002.2581 [hep-ph]].
[75] C. Bierlich, S. Chakraborty, N. Desai, L. Gellersen, I. Helenius, P. Ilten, L. Lönnblad, S. Mrenna, S. Prestel and C. T. Preuss, et al. [arXiv:2203.11601 [hep-ph]].
[76] T. J. Hou, K. Xie, J. Gao, S. Dulat, M. Guzzi, T. J. Hobbs, J. Huston, P. Nadolsky, J. Pumplin and C. Schmidt, et al. [arXiv:1908.11394 [hep-ph]].
[77] M. Cacciari, G. P. Salam and G. Soyez, Eur. Phys. J. C 72 (2012), 1896 [arXiv:1111.6097 [hep-ph]].
[78] S. Wang, W. Dai, B. W. Zhang and E. Wang, Eur. Phys. J. C 79 (2019) no.9, 789 [arXiv:1906.01499 [nucl-th]].
[79] S. Wang, W. Dai, J. Yan, B. W. Zhang and E. Wang, Nucl. Phys. A 1005 (2021), 121787 [arXiv:2001.11660 [nucl-th]].
[80] S. Wang, W. Dai, B. W. Zhang and E. Wang, Chin. Phys. C 45 (2021) no.6, 064105 [arXiv:2012.13935 [nucl-th]].
[81] S. Wang, W. Dai, B. W. Zhang and E. Wang, PoS HardProbes2020 (2021), 097 [arXiv:2009.13959 [nucl-th]].
[82] S. Wang, W. Dai, B. W. Zhang and E. Wang, Chin. Phys. C 47 (2023) no.5, 054102 [arXiv:2005.07018 [hep-ph]].
[83] S. Wang, J. W. Kang, W. Dai, B. W. Zhang and E. Wang, Eur. Phys. J. A 58 (2022) no.7, 135 [arXiv:2107.12000 [nucl-th]].
[84] Y. Li, S. Wang and B. W. Zhang, Phys. Rev. C 108 (2023) no.2, 2 [arXiv:2209.00548 [hep-ph]].
[85] S. Wang, Y. Li, S. Shen, B. W. Zhang and E. Wang, [arXiv:2308.14538 [hep-ph]].
[86] X. f. Guo and X. N. Wang, Phys. Rev. Lett. 85, 3591-3594 (2000) [arXiv:hep-ph/0005044 [hep-ph]].
[87] B. W. Zhang and X. N. Wang, Nucl. Phys. A 720, 429 (2003).
[88] A. Majumder, Phys. Rev. D 85, 014023 (2012) [arXiv:0912.2987 [nucl-th]].
[89] W. t. Deng and X. N. Wang, Phys. Rev. C 81 (2010) 024902 [arXiv:0910.3403 [hep-ph]].
[90] X. F. Chen, C. Greiner, E. Wang, X. N. Wang and Z. Xu, Phys. Rev. C 81 (2010), 064908 [arXiv:1002.1165 [nucl-th]].
[91] S. Acharya et al. [ALICE], Phys. Lett. B 804 (2020), 135377 [arXiv:1910.09110 [nucl-ex]].
[92] X. Dong, Y. J. Lee and R. Rapp, Ann. Rev. Nucl. Part. Sci. 69 (2019), 417-445 [arXiv:1903.07709 [nucl-ex]].
[93] R. B. Neufeld, Phys. Rev. D 83 (2011), 065012 [arXiv:1011.4979 [hep-ph]].
[94] J. Huang, Z. B. Kang and I. Vitev, Phys. Lett. B 726 (2013), 251-256 [arXiv:1306.0909 [hep-ph]].
[95] L. G. Pang, H. Petersen, Q. Wang and X. N. Wang, Phys. Rev. Lett. 117 (2016) no.19, 192301 [arXiv:1605.04024 [hep-ph]].
[96] L. G. Pang, H. Petersen and X. N. Wang, Phys. Rev. C 97 (2018) no.6, 064918 [arXiv:1802.04449 [nucl-th]].
[97] A. Banfi, G. P. Salam and G. Zanderighi, Eur. Phys. J. C 47 (2006), 113-124 [arXiv:hep-ph/0601139 [hep-ph]].
[98] M. Czakon, A. Mitov and R. Poncelet, JHEP 04 (2023), 138 [arXiv:2205.11879 [hep-ph]].
[99] R. Gauld, A. Huss and G. Stagnitto, Phys. Rev. Lett. 130 (2023) no.16, 161901 [arXiv:2208.11138 [hep-ph]].
[100] F. Caola, R. Grabarczyk, M. L. Hutt, G. P. Salam, L. Scyboz and J. Thaler, Phys. Rev. D 108 (2023) no.9, 094010 [arXiv:2306.07314 [hep-ph]].
[101] T. Sjostrand, S. Mrenna and P. Z. Skands, JHEP 05 (2006), 026 [arXiv:hep-ph/0603175 [hep-ph]].